nature photonics

LETTERS

https://doi.org/10.1038/s41566-018-0213-5

A phonon laser operating at an exceptional point

Jing Zhang[1,2,3,10], Bo Peng[1,8,10], Şahin Kaya Özdemir[1,9], Kevin Pichler[4], Dmitry O. Krimer[4], Guangming Zhao[1], Franco Nori[5,6], Yu-xi Liu[3,7], Stefan Rotter[4] and Lan Yang[1*]

Non-Hermitian physical systems have attracted considerable attention lately for their unconventional behaviour around exceptional points (EPs)—spectral singularities at which eigenvalues and eigenvectors coalesce. In particular, many new EP-related concepts such as unidirectional lasing and invisibility, as well as chiral transmission, have been realized. Given the progress in understanding the physics of EPs in various photonic structures, it is surprising that one of the oldest theoretical predictions associated with them, a remarkable broadening of the laser linewidth at an EP, has been probed only indirectly so far. Here, we fill this gap by steering a phonon laser through an EP in a compound optomechanical system formed by two coupled resonators. We observe a pronounced linewidth broadening of the mechanical lasing mode generated in one of the resonators when the system approaches the EP.

Non-Hermitian systems featuring EPs have attracted attention in many fields of physics[1,2]. In particular, there has been an increasing number of experiments in recent years that have not only demonstrated unique properties of EPs, such as the topology of self-intersecting Riemann sheets around them[3,4], but also led to proposals of practical applications based on features associated with EPs, such as loss-induced transmission and unidirectional invisibility[5–11], chiral behaviour[12], mode selection in lasers[13–15], enhanced sensors[16–19] and topological energy transfer[3,20]. A special share of attention has been dedicated to EPs in parity–time symmetric systems, where resonant or guided modes can be efficiently controlled by sweeping them across an EP[5–7].

Historically, one of the first predictions associated with EPs is the extreme broadening of the laser linewidth[21,22] beyond the fundamental Schawlow–Townes limit[23]. This broadening is quantified by the Petermann factor[24,25], which measures the excess quantum noise induced by the non-orthogonality of resonator modes. Specifically, the coupling between modes, induced by the openness of the resonator and the internal dissipation, is translated into excess noise by the gain mechanism and the cavity feedback[26]. Although early work showed that this linewidth broadening due to non-orthogonal resonator modes can, indeed, be measured[27–29], only subsequent theoretical work associated a pronounced linewidth enhancement in unstable laser resonators with the presence of a nearby EP[22]. What really happens to the linewidth when a laser operates at an EP has remained unclear to this day. Standard laser theory[24,25] and general arguments based on self-orthogonality of modes[2] predict an unphysical divergence of the laser linewidth at the EP[21,30,31] where modes coalesce and become completely non-orthogonal (that is, parallel). More recent theoretical models provide a more consistent framework for calculating the laser linewidth[32–35] but fail to resolve the problems directly at the EP. Experimentally, it is not straightforward to steer a laser directly to an EP[13,36,37] nor to measure its extremely narrow linewidth. Additionally, laser modes have a tendency to become unstable close to an EP where the spectral vicinity of a second mode may lead to chaotic lasing that could be wrongly perceived as an extremely broad laser line.

Here, we provide a new strategy to tackle this problem by working with a phonon laser rather than with its optical counterpart. Phonon lasers that produce coherent sound oscillations (mechanical vibrations) induced by optical pumping have been introduced recently[38], and have been studied theoretically within the framework of parity–time symmetry and EP physics with many interesting predictions, such as thresholdless phonon lasing[39]. For a study of lasing at an EP, phonon lasers have the crucial advantage that the linewidth measurement is much easier than for an optical laser. Moreover, as we will discuss below, the phonon laser considered in this study provides an interesting platform to study EPs in atomic spectra[40].

The concept of the phonon laser used here is based on a system developed by Grudinin, Vahala and co-workers[38], who showed that a system of two coupled optical microresonators, one of which supports a mechanical mode, can produce coherent mechanical oscillations with characteristics that are typical for photon lasers, such as a threshold, a linewidth narrowing above threshold, and nonlinear saturation effects. To drive the mechanical mode resonantly, the frequency difference of the two optical supermodes formed through inter-resonator coupling is matched with the frequency of the mechanical mode. In analogy to a photon laser, here the two optical supermodes correspond to the ground and excited states of an atomic two-level system, and the mechanical mode (phonons) mediates the transition between them. The energy difference between the optical supermodes can be finely tuned, either by changing the distance between the resonators or by introducing additional loss to the resonator without the mechanical mode, such that the spectrum exhibits an EP. Therefore, this configuration provides an interesting platform on which to study not only lasing at an EP but also EPs in atomic spectra[40] (the two-level system here). In this sense, phonon lasing in this tunable 'two-level system' also brings in new conceptual aspects as compared with recent studies of EPs in photonic lasers in which EPs emerged owing to the overlapping of cavity modes while the energy levels of the gain material were kept fixed (here these roles are exchanged).

Our experimental platform is a compound optomechanical system composed of two coupled silica whispering-gallery-mode

[1]Department of Electrical and Systems Engineering, Washington University, St Louis, MO, USA. [2]Department of Automation, Tsinghua University, Beijing, China. [3]Center for Quantum Information Science and Technology, BNRist, Beijing, China. [4]Institute for Theoretical Physics, Vienna University of Technology (TU Wien), Vienna, Austria. [5]Theoretical Quantum Physics Laboratory, RIKEN, Saitama, Japan. [6]Physics Department, The University of Michigan, Ann Arbor, MI, USA. [7]Institute of Microelectronics, Tsinghua University, Beijing, China. [8]Present address: IBM Thomas J. Watson Research Center, Yorktown Heights, NY, USA. [9]Present address: Department of Engineering Science and Mechanics, The Pennsylvania State University, University Park, PA, USA. [10]These authors contributed equally: Jing Zhang, Bo Peng. *e-mail: yang@seas.wustl.edu

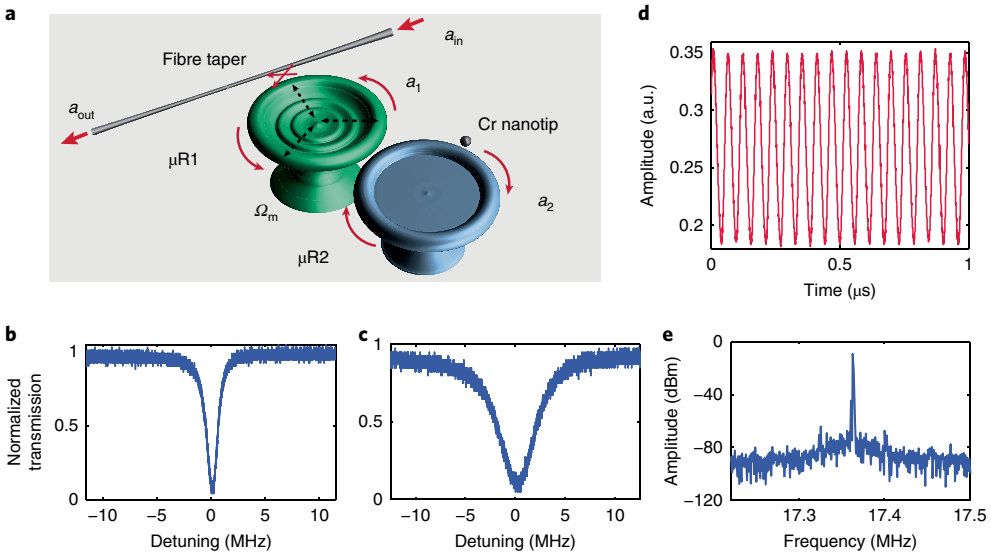

Fig. 1 | Phonon lasing in a compound resonator system. a, Schematic diagram of the compound phonon-laser system. Two microtoroid resonators, μR1 and μR2, are coupled to each other by evanescent fields. The first resonator μR1 supports a high-*Q* optical mode a_1 and a mechanical mode with resonance frequency Ω_m. The second resonator μR2 supports a low-*Q* optical mode a_2, and the damping rate of this low-*Q* mode can be tuned by a chromium-coated silica nanotip approaching μR2. **b**,**c**, Transmission spectra of the high-*Q* optical mode a_1 (**b**) and the low-*Q* optical mode a_2 (**c**) that exhibit Lorentzian lineshapes. **d**, Periodic time evolution of the mechanical mode supported by the resonator μR1. **e**, Radiofrequency spectrum of the mechanical mode in the phonon lasing regime.

microresonators (Fig. 1a) μR1 and μR2, where only the resonator μR1 supports a mechanical mode with frequency $\Omega_m = 17.38$ MHz and mechanical damping rate $\Gamma_m = 40$ kHz (measured just below the oscillation threshold). To optically excite the mechanical mode for phonon lasing, as well as to characterize the optical and mechanical modes, light from a tunable laser was coupled into μR1 by means of a tapered fibre, which was also used to out-couple the light from μR1 and direct it to a detector. The quality factors (Q) of the optical modes of μR1 and μR2 were 6.33×10^7 and 1.5×10^7, respectively. Typical transmission spectra obtained when the resonators were probed individually are given in Fig. 1b,c.

To steer the system towards or away from its EP, and to observe the behaviour of phonon lasing in the vicinity of an EP, we introduced additional loss to μR2 using a chromium-coated silica nanofibre tip (Fig. 1a), which has strong absorption in the 1,550-nm band. This additional loss, characterized by the damping rate γ_{tip}, was adjusted by increasing the overlap of the nanotip with the evanescent field of μR2. By introducing this extra loss for the optical modes, we tune the decay rates of the optical supermodes as well as their frequency difference, which then affect the interaction between the mechanical sound wave and this 'two-level system'. We used the thermo-optic effect to tune the resonance frequencies of the resonators to be the same before they were coupled. The inter-resonator distance was finely adjusted to control the coupling strength between the resonators, which induced the formation of two supermodes, and enabled efficient excitation of the mechanical mode, and hence of phonon lasing, when the spectral distance between the two supermodes was equal to the frequency of the mechanical mode supported in μR1. When this compound system was driven by an optical field with power above a certain threshold value, radiation-pressure-induced mechanical oscillations set in, leading to the modulation of the transmitted light at the frequency Ω_m of the mechanical motion (Fig. 1d). The radiofrequency (RF) spectrum of the modulated light provides information on the mechanical mode which is revealed by the peak located at Ω_m (Fig. 1e).

In the absence of the mechanical mode, the coupling between the optical modes a_1 of μR1 (the resonator supporting the mechanical motion) and a_2 of μR2 (the resonator without the mechanical motion) having the same frequency ω_0 creates two optical supermodes $a_\pm$ with complex eigenfrequencies $\omega_\pm = \omega_0 - i\chi \pm \beta$ where $\chi = (\gamma_1+\gamma_2)/2$ and $\beta = \sqrt{\kappa^2-\gamma^2}$ with $\gamma = (\gamma_2-\gamma_1)/2$. Here, κ is the coupling strength between the modes, $\gamma_1 = \gamma_{10}+\gamma_{c1}$ and $\gamma_2 = \gamma_{20}+\gamma_{tip}$ are the damping rates of the optical modes a_1 and a_2 with γ_{10} and γ_{20} representing their intrinsic damping rates, and γ_{c1}, γ_{tip} denote, respectively, the coupling loss of the taper–μR1 system and the additional loss introduced to μR2 by the nanotip. The point ($\kappa=\gamma$), where the eigenvalues of the system coalesce at $\omega_\pm = \omega_0 - i\chi$, corresponds to an EP at which the eigenvectors also coalesce. In the region before the EP ($\kappa>\gamma$), the supermodes have the same damping rate χ but different resonance frequencies $\omega_\pm = \omega_0 \pm \beta$ separated from each other by 2β. In the region after the EP ($\kappa<\gamma$), the supermodes have the same frequency ω_0 but different damping rates $\chi \mp i\beta$. In our experiments, where the coupling strength κ determined by the physical distance between the resonators was kept fixed, γ_{tip} was tuned to vary γ, which in turn allowed us to operate the system in three different regimes (before, after, and in the vicinity of the EP). From the experimentally obtained transmission spectra, we estimated the relevant parameters as $\kappa = 12.63$ MHz, $\gamma_{10} = 1.58$ MHz, $\gamma_{20} = 13.56$ MHz and $\gamma_{c1} = 1.58$ MHz.

Our experiments and the underlying physics of phonon lasing at an EP can be intuitively understood as follows (Fig. 2). Initially, the system is in the strong coupling regime (that is, before the EP) and the spectra exhibit two well-separated resonant modes (located at $\omega_\pm = \omega_0 \pm \beta$ with a spectral splitting of $2\beta \approx \Omega_m$), which are symmetrically distributed in the resonators (Fig. 2a). When the power of the pump laser with its frequency set around $\omega_+ = \omega_0 + \beta$ is above the threshold of mechanical oscillation, this mechanical oscillation in μR1 creates Stokes and anti-Stokes scattered photons with frequency $\omega_S = \omega_0 - \beta$ and $\omega_{aS} = \omega_0 + 3\beta$, respectively. Because ω_S lies within the frequency band of the resonance at $\omega_- = \omega_0 - \beta$, the amplitude of the Stokes sideband is resonantly enhanced. The amplitude of the anti-Stokes sideband, on the other hand, is suppressed because of the absence of a resonance at ω_{aS}. As a result, energy flows from photons to phonons in a highly efficient way due to resonantly enhanced

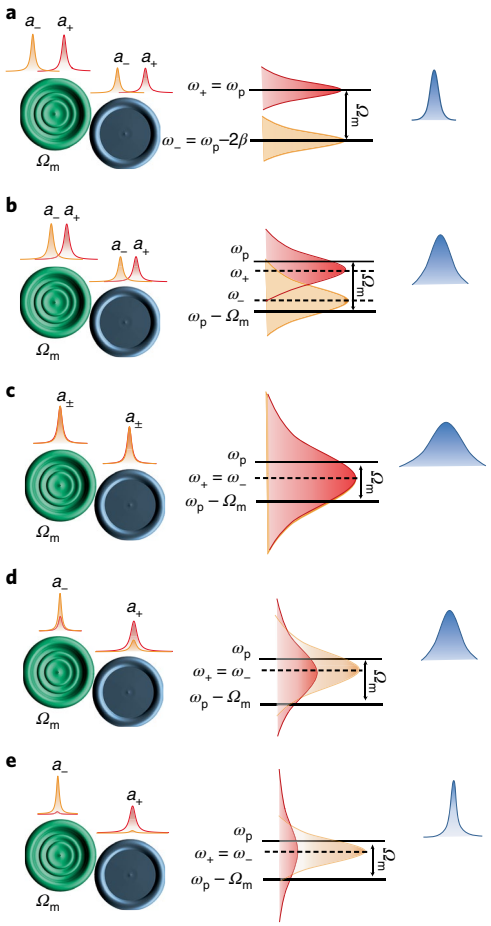

Fig. 2 | Tuning a phonon laser to an exceptional point. The first column shows a schematic of the distribution of the optical supermodes $a_\pm$ in the two resonators. The second column illustrates the frequency difference and linewidths of the two optical supermodes $a_\pm$. The last column represents the linewidth of the phonon laser. The damping rate γ_{tip} increases from **a** to **e**. **a**,**b**, The regime before the EP: the pump mode and the Stokes mode, which act as the analogue of a two-level atom, are within the frequency bands of the two optical supermodes respectively. The increasing γ_{tip} leads to the increase of the linewidths of the optical supermodes and to the decrease of the frequency difference between them. **c**, The EP at which the two optical supermodes are degenerate, and the pump mode and the Stokes mode are within the frequency bands of these two optical supermodes. The non-orthogonality of the optical modes introduces excess noise in the optical modes that reaches a maximum at the EP. Driven by the optical modes, the phonon laser inherits the increased optical noise, which is reflected by a broadened mechanical linewidth. **d**,**e**, The regime after the EP: the pump mode and the Stokes mode are within the frequency bands of the optical supermodes a_- and a_+ that are localized in the first and second resonators, respectively. The increasing γ_{tip} pushes the system away from the EP, leading to a linewidth narrowing of the phonon laser.

pumping of the system at ω_+ and resonantly enhanced collection of the Stokes photons at ω_-, resulting in coherent amplification of the mechanical oscillation. In this setting, the optical supermodes a_+ and a_- mimic a two-level system in which the transitions between the two levels are mediated by the mechanical mode, thereby creating a 'phonon laser'.

Introducing the nanotip, and hence inducing additional loss γ_{tip}, to μR2 moves the two supermodes spectrally closer to each other. Therefore, with increasing γ_{tip}, the system transits from well-separated and symmetrically distributed supermodes (Fig. 2a) to increasingly overlapping supermodes (Fig. 2b,c) with a complete overlap achieved at the EP (Fig. 2c). Further increase of γ_{tip} pushes the system beyond the EP, resulting in the strong localization of one of the supermodes in μR1 and the other in μR2 (Fig. 2d,e). Consequently, the mode in μR2 dissipates quickly owing to the presence of γ_{tip} while the mode in μR1 barely feels γ_{tip}. For the situation in which the supermodes overlap considerably (Fig. 2c–e), phonon lasing takes place because the resulting linewidth broadening of the overlapping modes is larger than the frequency of the mechanical mode. In the picture of a two-level system, this whole process corresponds to tuning the energy difference between the upper and lower energy levels such that with increasing γ_{tip} the upper and lower levels approach each other and become degenerate at an EP. As a result, during this process both the threshold and the linewidth of the phonon laser are affected (see our detailed discussion based on the experimental results below). First, increasing loss redistributes the supermodes between the resonators and alters the intracavity field intensity in μR1[13], which supports the mechanical mode, leading to a variation of the phonon lasing threshold such that the threshold first increases and then decreases as the system moves closer to the EP (Fig. 3). Second, the emitter (upper level) and collector (lower level) states are completely overlapping and non-orthogonal at the EP such that the enhancement of the noise in the optical modes becomes maximal. The noise inherent in these optical modes imprints on the phonon mode a linewidth that is maximally broadened at the EP (Fig. 4).

The behaviour of the phonon lasing threshold discussed above is seen in our experiments. Figure 3a depicts the RF signal power versus the optical pump power obtained at various values of γ_{tip}. In Fig. 3b, we present the threshold values as a function of the loss induced by the tip (that is, γ_{tip}). This shows that when γ_{tip} is increased, the threshold of the phonon laser first increases very slowly; after reaching a maximum value at a critical value of γ_{tip}, the threshold experiences a sudden drop. This behaviour is due to the loss-induced redistribution of the supermodes $a_\pm$ in the two resonators μR1 and μR2 when the system approaches the EP: in particular, when we increase the loss γ_{tip} such that the system approaches the EP, the intracavity field intensity in the high-Q resonator μR1 will first decrease to reach a minimum and then increase[13]. Because the phonon mode is located in the high-Q resonator μR1, this increase means that more energy can be transferred from the optical modes to the phonon mode for fixed input pump power such that the threshold of the phonon laser is decreased.

Next we focus on the central question: how is the linewidth of the phonon laser affected when it is operated near or at an EP? As shown in Fig. 4a, when the phonon laser was operated under different values of γ_{tip} while the pump power was tuned to keep the RF peak power of the phonon laser fixed, the linewidth of the phonon laser first increased in the regime before the EP but then decreased when the loss was further increased to move the system beyond the EP (into the regime after the EP). The phonon laser studied here is an analogue to a photon laser, but where, however, the lower and upper levels of a gain medium are replaced by two optical supermodes, and the photon-mediated transitions between the two levels are replaced by phonon-mediated transitions[38]. As discussed in detail in the Supplementary Information, the linewidth of the phonon laser can be calculated and represented in a similar way to a photon laser by taking into account the noise-induced phase diffusion process, resulting in the following approximate expression for the linewidth of the phonon laser

$$\Delta\nu \approx \Delta\nu_0 + \frac{\Gamma_m}{2n_{b,ss}}(2n_{spon} + 2n_{bT} + 1) \quad (1)$$

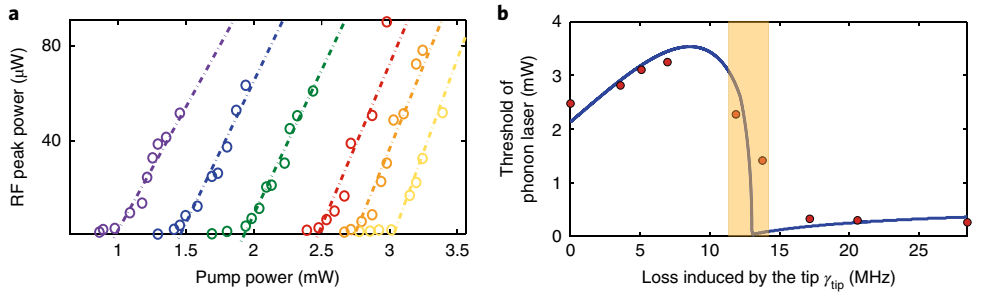

Fig. 3 | The threshold of the phonon laser before and after the exceptional point. a, Threshold curves of the phonon laser for different γ_{tip}. The damping rates for the threshold curves from left to right are γ_{tip} = 17.2 MHz, 13.8 MHz, 11.9 MHz, 0 MHz, 3.8 MHz and 6.9 MHz. **b**, The threshold of the phonon laser versus γ_{tip}. Before the EP, the threshold of the phonon laser increases with the increase of γ_{tip}, and then experiences a sudden drop in the vicinity of the EP. After the EP, the threshold of the phonon laser monotonously increases with the increase of γ_{tip}. The orange shaded area shows the region in the vicinity of the EP.

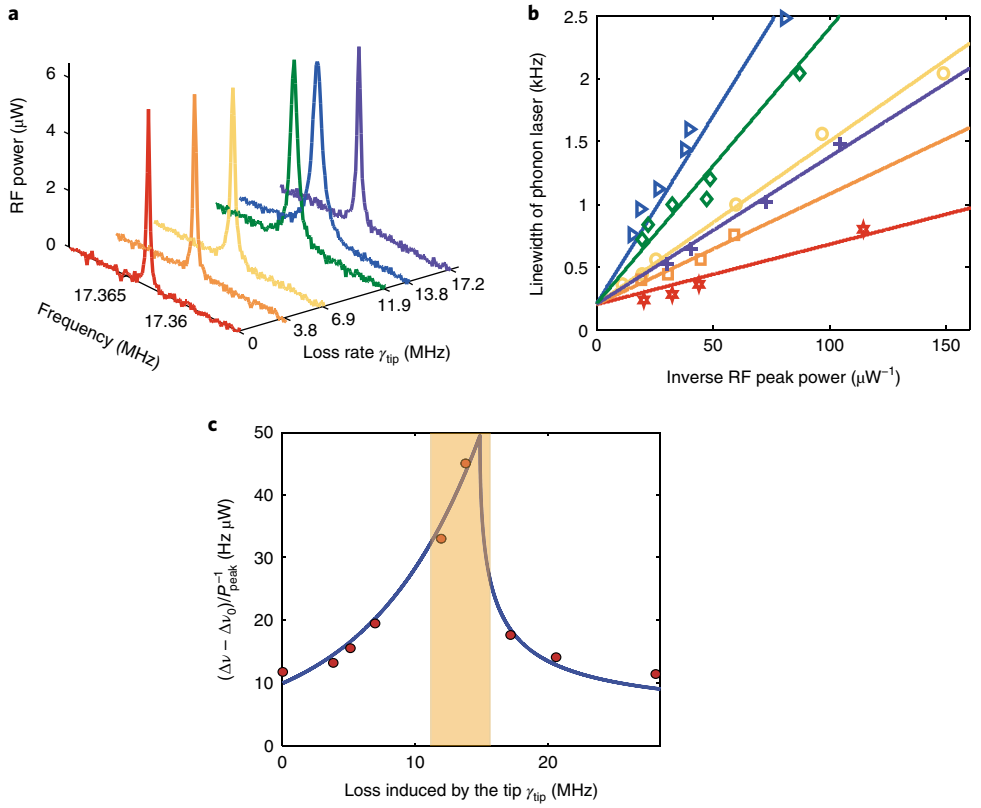

Fig. 4 | Linewidth enhancement of a phonon laser at an exceptional point. a, The power spectra of the phonon laser at different damping rates γ_{tip}. The linewidth of the phonon laser first increases and then decreases when we increase γ_{tip} from 0 MHz to 17.2 MHz. **b**, Linewidth versus inverse RF peak power of the phonon laser. Different curves correspond to different γ_{tip}. All the curves start from the same point with non-zero linewidth but feature different slopes. The damping rates for the curves from top to bottom are γ_{tip} = 13.8 MHz, 11.9 MHz, 6.9 MHz, 17.2 MHz, 3.8 MHz and 0 MHz. **c**, The red circles and the blue solid curve denote the experimental data points and a guide to the eye of the ratio between the normalized linewidth of the phonon laser and the inverse of the RF peak power $(\Delta\nu - \Delta\nu_0)/P_{peak}^{-1}$, which is enhanced in the vicinity of the EP (orange shaded area).

where $n_{b,ss}$ is the steady-state number of phonons, which is proportional to the RF peak power of the phonon laser P_{peak}, and $\Delta\nu_0$ is a phenomenological linewidth contribution taking into account all power-independent noise sources that are not included in our model. The factor n_{bT} represents the thermally excited phonons, and n_{spon} has been introduced in analogy to what is adopted in conventional laser theory, where it represents the number of spontaneously emitted photons into the cavity. In our phonon laser system, this factor n_{spon} is strongly enhanced when approaching the EP owing to the increasing noise in the optical supermodes, thereby creating a growing number of incoherent phonons in the mechanical resonator, which broaden the laser line (see the Supplementary Information for more details). We emphasize, however, that this increase of the linewidth in the vicinity of the EP has a different origin from that of a similar increase predicted for the photon laser. In the latter, the EP emerges because of overlapping modes of the optical resonator. In the phonon laser studied here, the EP emerges in the two-level system (that is, optical supermodes of the system)

where the transitions are mediated by phonons (that is, a mechanical mode). Quite remarkably, however, in both of these cases the EP leads to a considerable linewidth enhancement.

The linear dependence of the phonon laser linewidth $\Delta\nu$ on its inverse RF peak power (P_{peak}^{-1} proportional to $n_{\mathrm{b,ss}}^{-1}$) (see equation (1)) is clearly seen in our experimental results (Fig. 4b). In the limit of zero inverse output power $P_{\mathrm{peak}}^{-1} \to 0$ (that is, for strong output power), the linewidth $\Delta\nu$ approaches $\Delta\nu_0$, which is reflected in our experiments by the fact that for all different values of γ_{tip}, we found the same value of a power-independent linewidth $\Delta\nu_0 \approx 0.2\,\mathrm{kHz}$. As seen in Fig. 4c, the linewidth enhancement factor of the phonon laser given by $(\Delta\nu - \Delta\nu_0)/P_{\mathrm{peak}}^{-1}$ increases significantly as γ_{tip} is increased and the system moves closer to the EP. After passing the EP, the linewidth enhancement decreases again with further increase in γ_{tip}. For fixed RF peak power, we find that the linewidth of the phonon laser is enhanced at least five-fold at the EP. The underlying physics of this interesting behaviour can be understood as follows: when the system is steered towards the EP, the optical supermodes converge to each other, becoming more and more non-orthogonal until they are fully parallel at the EP. As can be shown in a simple scattering matrix model[26], the non-orthogonality of the optical modes leads to a marked increase of the effective optical noise and with it to a broadening of the optical linewidth (as inherent in the Petermann factor) that reaches a maximum directly at the EP (see the Supplementary Information for details). As, in our system, the phonon mode is driven by these noisy optical modes, the increased optical noise transfers directly to a mechanical excess noise and consequently leads to a broadening of the mechanical linewidth. In this sense, the phononic mode in our set-up may be interpreted as a probe of the optical noise in the optical supermodes. While these results imply that the coherence of the phonon laser is decreased in the vicinity of an EP, they also show that one can tune the linewidth of the phonon laser by moving it closer to or away from an EP. This may be useful for applications in which the linewidth or coherence of the phonon laser are of importance.

This work differs from ref.[13] in many ways, in particular in the physical mechanism behind the observations, although in both cases the system is brought to the vicinity of an EP by additionally introduced losses. The most relevant differences are the following. First, ref.[13] considers a Raman laser (optical photons with a frequency in the terahertz regime) whereas the current work considers a phonon laser (amplification of mechanical mode, and phonons in the megahertz frequency regime). Second, in ref.[13] the gain for the laser is provided by the Raman process in silica, and the additionally induced loss does not affect the gain mechanism; it just redistributes the energy between supermodes by bringing the coupled resonator system to and away from an EP. In this work, the additional loss does affect the gain medium, by bringing the two-level system (the gain system) to and away from an EP where the energy levels of the two-level system coalesce. Thus, whereas in ref.[13] the EP emerges in the optical modes driving the gain mechanism, in this work the EP emerges in the spectra of the gain medium. Third, ref.[13] reports loss-induced suppression and revival of a Raman laser before and after an EP without any reference to the effect of the EP on the linewidth of the Raman laser. The current work, on the other hand, focuses on the effect of an EP on the linewidth of a phonon laser and reports the observation of linewidth broadening in this new context.

In summary, we have experimentally investigated a phonon laser to provide insights into the long-debated issue of how a laser—in particular its linewidth—is affected when being operated at an EP. By steering the phonon laser close to the EP, we have shown that its linewidth is greatly enhanced. This broadening is attributed to the increased noise in the two optical supermodes that provide the gain for the phonon laser and that increasingly overlap when approaching the EP. Our study provides direct experimental evidence showing that EP-enhanced optical noise can be transferred directly to mechanical noise, leading to a linewidth broadening in phonon lasers. It opens up new perspectives for the relation between noise and non-Hermitian physics and may find applications in various related fields such as signal processing technologies. For example, our system could be used as an on-chip phononic device, similar to fully integrated photonic devices, which are widely used for information processing. Even more interestingly, the studied platform can provide insight into EPs in two-level or multi-level systems and into their detection and control.

Data availability. The data that support the plots within this paper and other findings of this study are available from the corresponding author upon reasonable request.

Received: 14 August 2017; Accepted: 7 June 2018;
Published online: 09 July 2018

References

1. Bender, C. M. Making sense of non-Hermitian Hamiltonians. *Rep. Prog. Phys.* **70**, 947–1018 (2007).
2. Moiseyev, N. *Non-Hermitian Quantum Mechanics* (Cambridge Univ. Press, Cambridge, 2011).
3. Doppler, J. et al. Dynamically encircling an exceptional point for asymmetric mode switching. *Nature* **537**, 76–79 (2016).
4. Dembowski, C. et al. Experimental observation of the topological structure of exceptional points. *Phys. Rev. Lett.* **86**, 787–790 (2001).
5. Guo, A. et al. Observation of PT-symmetry breaking in complex optical potentials. *Phys. Rev. Lett.* **103**, 093902 (2009).
6. Rüter, C. E. et al. Observation of parity–time symmetry in optics. *Nat. Phys.* **6**, 192–195 (2010).
7. Klaiman, S., Günther, U. & Moiseyev, N. Visualization of branch points in PT-symmetric waveguides. *Phys. Rev. Lett.* **101**, 080402 (2008).
8. Lin, Z. et al. Unidirectional invisibility induced by PT-symmetric periodic structures. *Phys. Rev. Lett.* **106**, 213901 (2011).
9. Regensburger, A. et al. Parity–time synthetic photonic lattices. *Nature* **488**, 167–171 (2012).
10. Peng, B. et al. Parity–time-symmetric whispering-gallery microcavities. *Nat. Phys.* **10**, 394–398 (2014).
11. Chang, L. et al. Parity–time symmetry and variable optical isolation in active–passive-coupled microresonators. *Nat. Photon.* **8**, 524–529 (2014).
12. Peng, B. et al. Chiral modes and directional lasing at exceptional points. *Proc. Natl Acad. Sci. USA* **113**, 6845–6850 (2016).
13. Peng, B. et al. Loss-induced suppression and revival of lasing. *Science* **346**, 328–332 (2014).
14. Feng, L., Wong, Z. J., Ma, R.-M., Wang, Y. & Zhang, X. Single-mode laser by parity–time symmetry breaking. *Science* **346**, 972–975 (2014).
15. Hodaei, H., Miri, M.-A., Heinrich, M., Christodoulides, D. N. & Khajavikhan, M. Parity–time-symmetric microring lasers. *Science* **346**, 975–978 (2014).
16. Wiersig, J. Enhancing the sensitivity of frequency and energy splitting detection by using exceptional points: application to microcavity sensors for single-particle detection. *Phys. Rev. Lett.* **112**, 203901 (2014).
17. Liu, Z.-P. et al. Metrology with PT-symmetric cavities: enhanced sensitivity near the PT-phase transition. *Phys. Rev. Lett.* **117**, 110802 (2016).
18. Chen, W., Özdemir, S. K., Zhao, G., Wiersig, J. & Yang, L. Exceptional points enhance sensing in an optical microcavity. *Nature* **548**, 192–196 (2017).
19. Hodaei, H. et al. Enhanced sensitivity at higher-order exceptional points. *Nature* **548**, 187–191 (2017).
20. Xu, H., Mason, D., Jiang, L. & Harris, G. E. Topological energy transfer in an optomechanical system with exceptional points. *Nature* **537**, 80–83 (2016).
21. Wenzel, H., Bandelow, U., Wunsche, H. J. & Rehberg, J. Mechanisms of fast self pulsations in two-section DFB lasers. *IEEE J. Quantum Electron.* **32**, 69–78 (1996).
22. Berry, M. Mode degeneracies and the Petermann excess-noise factor for unstable lasers. *J. Mod. Opt.* **50**, 63–81 (2003).
23. Schawlow, A. L. & Townes, C. H. Infrared and optical masers. *Phys. Rev.* **112**, 1940–1948 (1958).
24. Peterman, K. Calculated spontaneous emission factor for double-heterostructure injection lasers with gain-induced waveguiding. *IEEE J. Quantum Electron.* **QE-15**, 566–570 (1979).
25. Siegman, A. E. Excess spontaneous emission in non-Hermitian optical systems. I. Laser amplifiers. *Phys. Rev. A* **39**, 1253–1263 (1989).
26. Grangier, P. & Poizat, J. P. A simple quantum picture for the Petermann excess noise factor. *Eur. Phys. J. D* **1**, 97–104 (1998).
27. Hamel, W. A. & Woerdman, J. P. Observation of enhanced fundamental linewidth of a laser due to nonorthogonality of its longitudinal eigenmodes. *Phys. Rev. Lett.* **64**, 1506 (1990).

28. Cheng, Y.-J., Fanning, C. G. & Siegman, A. E. Experimental observation of a large excess quantum noise factor in the linewidth of a laser oscillator having nonorthogonal modes. *Phys. Rev. Lett.* **77**, 627–630 (1996).
29. van Eijkelenborg, M. A., Lindberg, Å. M., Thijssen, M. S. & Woerdman, J. P. Resonance of quantum noise in an unstable cavity laser. *Phys. Rev. Lett.* **77**, 4314–4317 (1996).
30. Schomerus, H., Frahm, K. M., Patra, M. & Beenakker, C. W. J. Quantum limit of the laser line width in chaotic cavities and statistics of residues of scattering matrix poles. *Phys. A* **278**, 469–496 (2000).
31. Lee, S.-Y. et al. Divergent Petermann factor of interacting resonances in a stadium-shaped microcavity. *Phys. Rev. A* **78**, 015805 (2008).
32. Yoo, G., Sim, H.-S. & Schomerus, H. Quantum noise and mode nonorthogonality in non-Hermitian PT-symmetric optical resonators. *Phys. Rev. A* **84**, 063833 (2011).
33. Schomerus, H. Excess quantum noise due to mode nonorthogonality in dielectric microresonators. *Phys. Rev. A* **79**, 061801(R) (2009).
34. Chong, Y. D. & Douglas Stone, A. General linewidth formula for steady-state multimode lasing in arbitrary cavities. *Phys. Rev. Lett.* **109**, 063902 (2012).
35. Pick, A. et al. Ab initio multimode linewidth theory for arbitrary inhomogeneous laser cavities. *Phys. Rev. A* **91**, 063806 (2015).
36. Liertzer, M. et al. Pump-induced exceptional points in lasers. *Phys. Rev. Lett.* **108**, 173901 (2012).
37. Brandstetter, M. et al. Reversing the pump dependence of a laser at an exceptional point. *Nat. Commun.* **5**, 4034 (2014).
38. Grudinin, I. S., Lee, H., Painter, O. & Vahala, K. J. Phonon laser action in a tunable two-level system. *Phys. Rev. Lett.* **104**, 083901 (2010).
39. Jing, H. et al. PT-symmetric phonon laser. *Phys. Rev. Lett.* **113**, 053604 (2014).
40. Cartarius, H., Main, J. & Wunner, G. Exceptional points in atomic spectra. *Phys. Rev. Lett.* **99**, 173003 (2007).

Acknowledgements

This work was supported by NSF grant no. EFMA1641109, ARO grant no. W911NF1210026, ARO grant no. W911NF1710189 and the European Commission under project NHQWAVE (MSCA-RISE 691209). S.K.O. was supported by ARO grant no. W911NF-16-1-0339. S.K.O thanks J. Mateo for his continuous support. J.Z. is supported by the NSFC under grant nos. 61622306, 11674194. Y.-X.L. is supported by the NSFC under grant no. 61025022. Y.-X.L. and J.Z. are supported by the National Basic Research Program of China (973 Program) under grant no. 2014CB921401, the Tsinghua University Initiative Scientific Research Program and the Tsinghua National Laboratory for Information Science and Technology (TNList) Cross-discipline Foundation. F.N. is partially supported by the MURI Center for Dynamic Magneto-Optics via AFOSR Award no. FA9550-14-1-0040, Asian Office of Aerospace Research and Development (AOARD) (grant no. FA2386-18-1-4045), the IMPACT program of JST, JSPS-RFBR grant no. 17-52-50023, CREST grant no. JPMJCR1676, RIKEN-AIST Joint Research Fund and the Sir John Templeton Foundation. K.P., D.O.K. and S.R. are supported by the Austrian Science Fund (FWF) through project no. SFB NextLite F49-P10. H. Yilmaz prepared the chromium-coated silica nanofibre tip for the experiments.

Author contributions

S.R., S.K.O, B.P. and L.Y. conceived the idea. B.P., J.Z., S.K.O., S.R. and L.Y. designed the experiments. J.Z and B.P. performed the experiments with help from G.Z. J.Z. analysed the experimental data, J.Z., K.P. and D.O.K. performed the theoretical analysis and numerical simulations, guided by S.K.O, Y.-X.L. and S.R. J.Z., S.K.O., S.R., Y.-X.L. and L.Y. wrote the manuscript with contributions from all authors. L.Y. supervised the research.

Competing interests

The authors declare no competing interests.

Additional information

Supplementary information is available for this paper at https://doi.org/10.1038/s41566-018-0213-5.

Reprints and permissions information is available at www.nature.com/reprints.

Correspondence and requests for materials should be addressed to L.Y.

Publisher's note: Springer Nature remains neutral with regard to jurisdictional claims in published maps and institutional affiliations.